THE INTERACTION OF LOCAL AND OVERALL BUCKLING OF THIN-WALLED STRUCTURES

A. van der Neut
Delft University of Technology
Department of Aeronautical Engineering
Delft, the Netherlands

Abstract

The commonly accepted criterion of optimization of thin structures that local and overall buckling loads should coincide overlooks the unfavourable effect of coupling between these two modes. The equilibrium at the local buckling load is instable over a range of the geometrical parameter R, which is the ratio between Euler en local buckling load, close to R = 1. Instable equilibrium yields imperfection sensitivity. Two imperfections are important: initial waviness of the composing plate strips and initial curvature of the axis of the structure.

Three models have been investigated: 1, the strut composed of 2 equal load carrying flanges; 2, the plate with stringers not affected by local buckling; 3, a simplified representation of a panel stiffened by top-hat stringers. The models 1 and 2 represent extreme conditions as to mode interaction: nr. 1 being highly imperfection sensitive; nr. 2 being subject to mode interaction only in a narrow range of R close to unity. These 2 cases have been investigated earlier. The purpose with the model nr. 3 is to explore the significance of mode interaction for the strength of heavily stiffened wing panels.

So as to avoid too great complexity the model is not identical to a real structure. However it incorporates the geometrical characteristic of the cross section: less material at the topside than at the plateside; and the characteristic of local buckling of these structures: elastic edge restraint of composing plate strips and equal wave length of their mode in spite of unequal strip widths.

The stiffness of imperfect plate strips under these conditions has been established and the results are used for determining the behaviour of the model. It appears that initial waviness reduces the strength close to R = 1. The equilibrium at the overall buckling load is instable up to R about 1,1. Consequently, some further reduction of the strength by initial curvature of the axis can be expected.

The strength of panels with R say up to 1,3 will scatter due to differences in imperfections. The amount of imperfection being unknown the strength of structures in this range of R cannot be established accurately by theory; several tests on identical specimen will be needed.

Symbols

K compressive force in the structure
L half of length of clamped structure
P compressive force in a single plate strip
R geometric parameter = K_E/K_ℓ
W deflection of longitudinal axis of the structure
b width of plate strip
h thickness of plate strip
j radius of gyration of the cross section
ℓ half wave length with local buckling
w deflection of plate strip
x,y longitudinal and lateral coordinates, resp.
α ratio of amplitude of strip imperfection to h
β ratio of amplitude of column axis imperfection to j
ε compressive strain of edge of strip
η stiffness reduction factor
$\lambda = \ell/b$
$\mu = \frac{1}{6}(2\eta'^2 - \eta\eta'')$
$\omega = w/h$

subscripts:
E refers to Euler buckling load
b refers to overall buckling load
ℓ refers to local buckling load
$()' = d(\ )/d(P/P_\ell)$

1. Introduction

When the compressive load per unit width is large, such as in wing panels, closely spaced stiffeners are needed. Then the local buckling stress is high and can be close to the overall (Euler) buckling stress. The optimal design seems to be reached when these buckling stresses coincide. Fig. 1 shows how the two stresses vary with varying width to thickness ratio b/h of the composing plate strips, the total cross section remaining constant. This figure suggests the location of the optimum. Upon further thought one might suspect that the optimum will be somewhat to the right of the intersection, considering that the load carrying capacity is not exhausted at the local buckling stress.

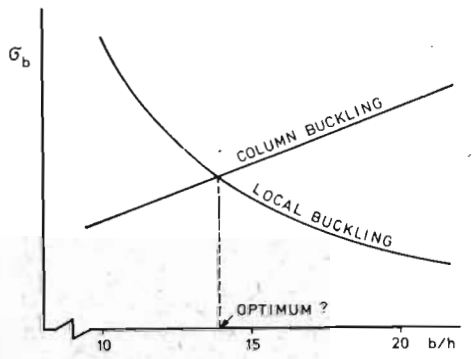

Figure 1. Apparent optimum design.

However these two buckling modes, both stable-highly stable in the case of local buckling; slightly stable as to overall buckling-, appear to interact. This interaction can cause severe instability at the buckling load. The consequence is similar to the behaviour of thin shells: the structure is sen-

sitive to imperfections. Imperfections reduce the load carrying capacity distinctly, which then depends on the size of the imperfections. These statements throw some light on two astonishing phenomen which happen to occur with panel tests: 1, the failure load is smaller than as well the local as the overall buckling load, as established from classical theory; 2, the panel collapses explosively.

The object of this paper is to warn designers for the unfavourable effect of mode interaction, to locate the dangerous area of the governing structural parameter and to give some quantitative idea of the strength reduction due to this effect.

The discussion starts with a model which is very sensitive to mode interaction. Next comes the other extreme: a panel where the stiffeners are not affected by local buckling. Finally an intermediate case will be discussed: a model which is representative for the behaviour of panels reinforced by tophatstringers.

Elastic behaviour has been assumed throughout.

2. Problem identification

A very sensitive structure is the strut, composed of two load carrying flanges[1]. Shear webs without longitudinal stiffness maintain the structural integrity (fig. 2). The upper figure shows the relation between compressive load P of the flange and its compressive strain ε. The graph has a kink at the local buckling load P_ℓ. From there on the reduction factor η of the longitudinal stiffness is 41%.

The lower figure depicts the Euler curve of column lengths above L_1. At L_1 the Euler load is equal to the local buckling load K_ℓ. When column failure occurs at a load K_b greater than K_ℓ the flanges are in the post-buckling state where their stiffness is reduced in the ratio η. Then the bending stiffness of the strut is equally reduced in the ratio η and the buckling load is $K_b = \eta K_E$, as shown by the curve to the left. It holds for column lengths smaller than L_2, at L_2 $K_b = K_\ell$.

It remains to establish how columns behave of length between L_1 and L_2. Up to K_ℓ the column remains straight. When a small deflection occurs the flange at the concave side passes into the post-buckling range. It reacts with its reduced stiffness. However the flange at the convex side remains in the unbuckled state (see upper part fig. 2). It reacts with the unreduced stiffness. Then the reduction factor of the bending stiffness of the strut is $2\eta/(1+\eta)$, which is 58%. At a certain length L_o this bending stiffness is just sufficient to maintain the strut in neutral equilibrium at infinitely small deflection.

When the column length is smaller than L_o, the strut is too stiff for the possibility of buckling. The strut is in stable equilibrium. However when the length is greater than L_o the strut is too long for being in equilibrium when deflected. It collapses explosively. These struts are at the load K_ℓ in instable equilibrium. Any disturbance, e.g. imperfection of the column axis, pushes the strength down below K_ℓ. This imperfection sensitivity increases with increasing column length and is maximal at the length L_1, where local and Euler buckling load coincide. Exactly the situation which according to fig. 1 seemed to be optimal.

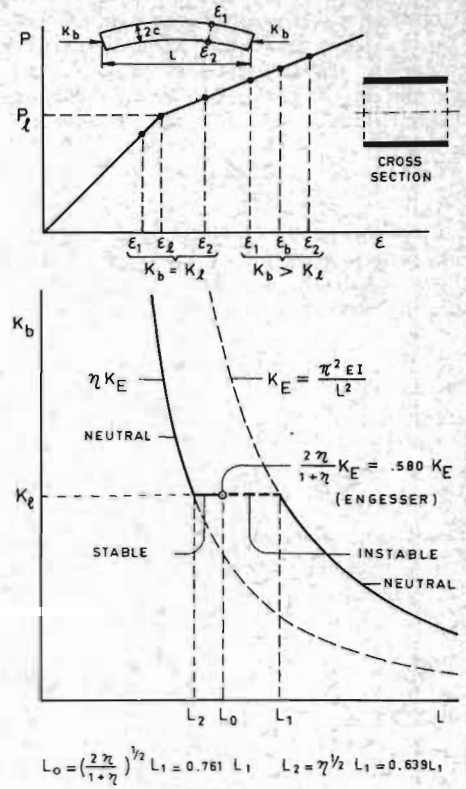

Figure 2. Column buckling load K_b against length L.

It is convenient to replace the abscissa L by L^{-2} or by $R = K_E/K_\ell$ so as to obtain a non-dimensional representation. Then fig. 2 transforms into fig. 3.

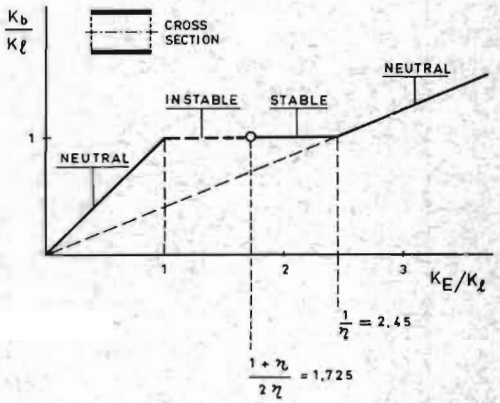

Figure 3. Column buckling load K_b against K_E.

3. The effect of imperfection of the flanges[1,2]

3.1. The buckling load K_b

The "flat" walls, composing a stiffened panel, are never flat in the mathematical sense. Depending on manufacturing they have more or less irregularity. When loaded in compression deflection occurs

before the local buckling stress is reached. The kink in the P-ε-curve disappears; the curve becomes a smooth line, which has its maximal deviation from the flat-wall-curve at ε_ℓ. In the vicinity of ε_ℓ the structure gives the maximal response to the component of the imperfection which has the shape of the local buckling mode. In order to get an idea of the effect of initial waviness only this component is being considered. Then with the two-flange-model the initial deflection is

$$w_o = a \sin \pi x/b \cos \pi y/b. \qquad (3.1)$$

Its amplitude is characterized by the non-dimensional parameter $\alpha = a/h$. Fig. 4 illustrates the kind of curve one obtains analytically [3].

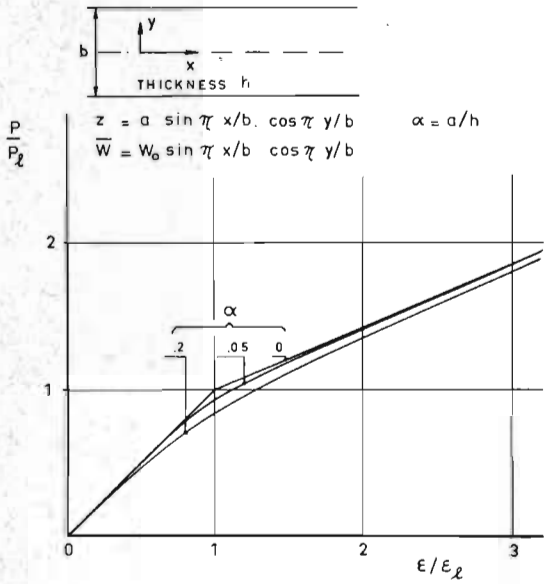

Figure 4. Load-strain curve of imperfect simply supported plate strip.

The stiffness of the flange against infinitesimal increment of the edge strains is $dP/d\varepsilon$. The reduction factor of the stifness is

$$\eta = d(P/P_\ell)/d(\varepsilon/\varepsilon_\ell). \qquad (3.2)$$

When the imperfection parameters of the two flanges are equal this η is also the reduction factor of the bending stiffness of the strut. Then its buckling load $K_b = \eta K_E$ or

$$\frac{1}{\eta_b}\frac{K_b}{K_\ell} = \frac{K_E}{K_\ell} = R = 3(1-\nu^2)\left(\frac{bc}{hL}\right)^2 \qquad (3.3)$$

This relation permits for any load parameter K/K_ℓ to establish the structural parameter R at which K is the buckling load. In this way one obtains the curves given in fig. 5.

It shows that with this model the buckling load is smaller than K_ℓ up to $K_E = 2K_\ell$. The maximal strength reduction occurs at $R = 1$. The "optimal" configuration appears to be the most sensitive one to imperfection. Even very small imperfection yields noticable reduction. The asymptotic solution by Koiter and Kuiken [4] yields that at $R = 1$ the reduction is proportional to $\alpha^{\frac{2}{3}}$.

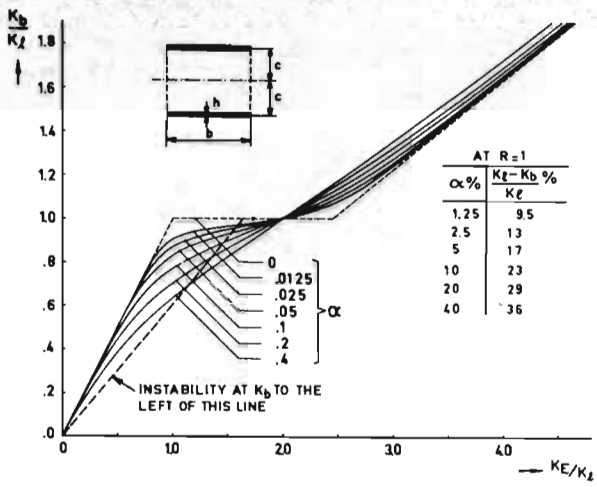

Figure 5. Buckling curves of columns with imperfect flanges.

Thompson and Lewis [5] have shown that the optimum more and more eroding with increasing imperfection moves from R = 1 to R < 1.

The tangent to the P-ε-curve represents the stiffness of the strut against infinitesimal strain increment. The K_b-K_E-relation so established means that the structure with the structural parameter R is in neutral equilibrium under the load K_b, however only with respect to infinitesimal deflection. At finite deflection the edge strains of the flanges ε_1 and ε_2 differ from ε_b by a finite amount. Since η is not constant but a function of ε the bending stiffness of the strut against finite deflection deviates from η_b EI. The non-linearity of the P-ε-curve introduces a non-linear problem. The question arises: is the strut still in equilibrium when the deflection is finite; is the load required for equilibrium smaller or greater than K_b? When the equilibrium load $K < K_b$, it means that the equilibrium of the undeflected strut is unstable and any casual deflection reduces the load carrying capacity. A strut is never mathematically straight. Any deviation from straightness of the column axis will affect the strength unfavourably.

Therefore the next problem to be considered is: how is the slope of the load-shortening curve at the bifurcation point K_b? Is the equilibrium at K_b stable, neutral or instable?

3.2. The character of the equilibrium at K_b

When the amplitude W_o of the column deflection is infinitesimal neutral equilibrium involves that

$$(dK/dW_o)_b = 0.$$

When W_o is finite the possibility exists that due to non-linearity

$$[dK/d(W_o)^2]_b \neq 0. \qquad (3.4)$$

Then in first approximation the compressive force which can be supported at small finite deflection is

$$K/K_\ell = K_b/K_\ell + t(W_o/2j)^2. \qquad (3.5)$$

The gradient $t = d(K/K_\ell)/d\,(W_o/2j)^2$ is to be established.

The condition for equilibrium in the deflected state is

$$\frac{d^2}{dx^2}\left[M + \left(K_b + K_\ell\, t\,(W_o/2j)^2\right)\right]W = 0 \qquad (3.6)$$

The last term of this equation is of the third degree in W. Then M has to be established as well up to terms of the third degree in W. This can be achieved by expressing the flange loads P as functions of $(\varepsilon-\varepsilon_b)$ up to the third degree term using the truncated Taylor expansion

$$P = P_b + \frac{dP}{d\varepsilon}(\varepsilon-\varepsilon_b) + \tfrac{1}{2}\frac{d^2P}{d\varepsilon^2}(\varepsilon-\varepsilon_b)^2 + \frac{1}{6}\frac{d^3P}{d\varepsilon^3}(\varepsilon-\varepsilon_b)^3 \qquad (3.7)$$

The flanges 1 and 2 have edge strains ε_1 and ε_2 resp., which are related to W by

$$\varepsilon_1-\varepsilon_2 = 2c\frac{d^2W}{dx^2}. \qquad (3.8)$$

The compressive force and the bending moment are resp.

$$K = P_1 + P_2, \qquad (3.9)$$

$$M = (P_1-P_2)c. \qquad (3.10)$$

The five equations (3-5, 7, 8, 9, 10) contain the seven unknown quantities t, ε_1, ε_2, P_1, P_2, M and W. Eliminating ε_1, ε_2, P_1, P_2 the result is the relation between M, W and t

$$M = \eta_b\, EI\,\frac{d^2W}{dx^2}\left[1-\mu_b\left(\frac{c}{\varepsilon_\ell}\right)^2\left(\frac{d^2W}{dx^2}\right)^2 + \left(\frac{\eta'}{\eta}\right)_b t\left(\frac{W_o}{2j}\right)^2\right], \qquad (3.11)$$

where

$$(\,)' = d(\,)/d(P/P_\ell) \text{ and } \mu = \frac{1}{6}(2\eta'^2 - \eta\eta'').$$

The expression between brackets is the multiplication factor of the bending stiffness η_b EI due to finite deflection. The bending stiffness appears to be function of x.

Using (3.11) the differential equation (3.6) in non-dimensional form, with $V = \frac{W}{2c} = \frac{W}{2j}$, is

$$\left\{V''\left[1 - 4\mu_b R^2 V''^2 + \left(\frac{\eta'}{\eta}\right)_b t\, V_o^2\right] + \left(1 + \frac{1}{\eta_b R}\, tV_o^2\right)V\right\}^{\cdot\cdot} = 0, \qquad (3.12)$$

where $(\,)^{\cdot} = \frac{L}{\pi}\frac{d(\,)}{dx}$.

This equation contains clearly third order terms in the small non-dimensional deflection V.

The solution of this equation is not unique; V_o the deflection in x = 0 is undetermined within the range of small but finite values. Substitution of the solution into (3.12) yields a left-hand-side, which is the sum op terms of the orders V_o, V_o^2 and V_o^3. Since V_o is undetermined each of these 3 terms must vanish, which yields 3 linear differential equations for the 3 components of V

$$V = V_1 + V_2 + V_3,$$

where V_1, V_2, V_3 are resp. of the order V_o, V_o^2, V_o^3.

Their solution for the column of length 2 L clamped at its ends is $V = V_{10}(\cos \pi x/L + 1) +$

$$+ \frac{1}{8}\mu_b R^2 V_{10}^3(\cos 3\pi x/L + 1). \qquad (3.13)$$

Further the differential equation stemming from the third order part yields

$$t = \left[\frac{d\,(K/K_\ell)}{d(W_o/2j)^2}\right]_b = -\frac{3}{4}\left(\frac{\eta\,\mu}{\frac{1}{R}-\eta'}\right)_b R^2. \qquad (3.14)$$

The tangent to the load-shortening curve in the bifurcation point K_b is

$$\frac{d(K/K_\ell)}{d(-\Delta L/L\varepsilon_\ell)} = \eta_b\left[1 - \frac{(\frac{1}{R}-\eta')^2}{3\mu}\right]_b^{-1}. \qquad (3.15)$$

Since η and $-\eta'$ are positive it follows from (3.14) that $t < 0$ in the range of K_b where $\mu > 0$. Over this range the equilibrium at K_b is unstable.

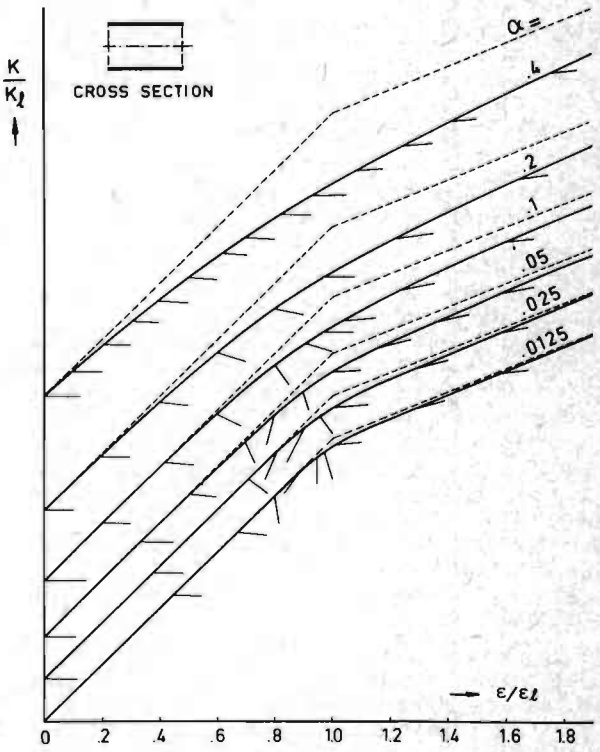

Figure 6. Load-strain curves and tangents to the load-shortening curves at the bifurcation load K_b.

Fig. 6 shows for a number of imperfections α the tangent to the load-shortening curve at the bifurcation, when K is the buckling load K_b. The instability is more severe with decreasing α. With small values of α it is maximal in the region of R between 0,9 and 1,0.

As remarked by Gilbert and Calladine[6], it follows from the formula of μ that for any value of α μ=0 when η = 0,608. This limit of the unstable region is in fig. 5 the straight interrupted line through the origin.

When the equilibrium is unstable a disturbance of the equilibrium causes explosive collapse at K_b. Non-straightness of the column axis reduces the failure load and, as can be expected, in correspondance with the severity of the unstability.

4. The effect of imperfection of the column axis

4.1. Initial curvature of the column axis[7]

The imperfection is chosen in the shape of the overall buckling mode, therefore

$$e = e_o (\cos \pi x/L + 1) \qquad (4.1)$$

Its amplitude e_o is characterized by the non-dimensional parameter $\beta = e_o/j$.

The problem is to establish the deflection W at any load K and more in particular to find the maximal load the strut can carry as a function of β and of the structural parameter R.

The differential equation of the strut is

$$\frac{d^2}{dx^2}\left[M + K\,(W + e)\right] = 0 .$$

M follows from (3.11) with t = 0 and η_b, μ_b replaced by η and μ pertaining to K/K_ℓ. The non-dimensional differential equation then is

$$\{V'' - 4\mu R^2 V''^3 + \frac{1}{\eta R} K/K_\ell \left[V + \tfrac{1}{2}\beta(\cos \pi x/L + 1)\right]\}'' = 0. \qquad (4.2)$$

With the preceding problem V could be decomposed in parts of different order due to the indeterminateness of V_o. In this case for any load below K_{max} there is a unique value of V_o. Then exact solution of V would require an infinite series. This however would do too much honour to eq. (4.2), which gives only an approximate description of the behaviour of the strut at finite deflections because it is based on a truncated Taylor expansion of P. This truncation accounts only for terms up to the third degree in V'' excluding terms of higher degree. The mechanical significance of the suppression of the higher order terms is that μ is considered to be constant in the range of strains occurring in the deflected state, however μ appears to vary quite distinctly, more in particular at small values of α. This is a consequence of the rapid change of the slope of the P-ε-curve near to ε_ℓ.

Therefore the solution obtained from (4.2) is approximative, only reliable at rather small deflection, therefore with small imperfection β. This approximate solution cannot indicate more than the trend of the effect of non-straightness of the strut. Under these conditions an approximate solution of the approxamating differential equation will do.

The solution for the strut clamped at its ends may then have the form $V = V_1(\cos \pi x/L + 1)$, where V_1 can be established by means of the Ritz-Galerkin method. This yields the equation

$$(1 - \frac{1}{\eta R}\frac{K}{K_\ell})\, V_1 - 3\mu R^2 V_1^3 = \frac{1}{2\eta R}\frac{K}{K_\ell}\,\beta . \qquad (4.4)$$

With constant K η and μ are constant. Then a given value of β yields 2 positive roots of V_1. With increasing β these 2 roots approach each other until they coincide. The corresponding value of β is the maximal imperfection at which the load K can be supported. Therefore this load is K_{max} for this imperfection β. When the roots coincide $d\beta/dV_1 = 0$, which yields

$$V_1 = \frac{1}{3R}\left[(1 - \frac{1}{\eta R}\frac{K}{K_\ell})/\mu\right]^{\frac{1}{2}} . \qquad (4.5)$$

Next from (4.4) follows the imperfection at which the column strength is limited to K.

$$\beta = \frac{4}{9}\,\eta\,\frac{K_\ell}{K}\left[(1 - \frac{1}{\eta R}\frac{K}{K_\ell})^3/\mu\right]^{\frac{1}{2}} . \qquad (4.6)$$

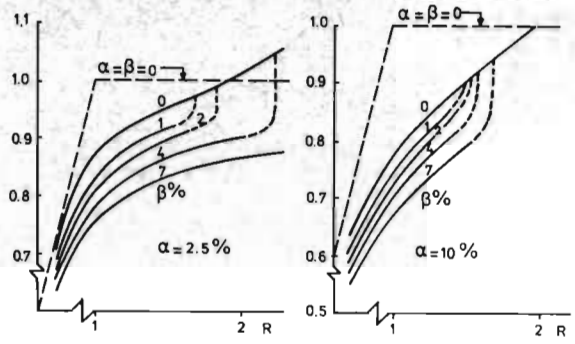

Figure 7. Strength reduction by imperfection of column axis.

Fig. 7 shows for a small and a large value of α the column strength as a function of the structural parameter R and for some values of the column imperfection β. With decreasing α and increasing β these data are less reliable.
The trends apparent from these curves are the following:

1. The effect of β is less than proportional to β. For small β the reduction of the strength is proportional to $\beta^{2/3}$.
2. The reduction is fairly constant over the range $0{,}8 < R < 1{,}6$.
3. The effect of β decreases with increasing α.
4. With large flange imperfections the strength reducing effect due to β is inferior to that by α.
5. With small flange imperfections the effects of α and β have comparable size. In the region of R = 1,5 the effect of β can even be predominant.

A recent investigation by Gilbert and Calladine[6] has brought more clarity on the relative importance of the two imperfections. They consider a model still more simple than the one considered up to here, a model which permits exact solutions. It consists of a strut composed of 2 stiff bars of equal length interconnected by a short deformable element of the two flange type. It appears that the reductions in the cases α = n, β = 0 and α = 0, β = n are about equal; the latter being slighter greater. Also the tendency appears that with increasing R the effect of β is greater than the effect of an equal value of α. The superpossition of the two imperfections increases the reduction only slightly in comparison to the effect of the imperfections considered separately; the increase is about constant in the range $0{,}8 < R < 1{,}6$.

These results appeal to the intuitive conjecture that the addition of another imperfection does less harm than the foregoing imperfection.

The investigation of the models considered so far has shown that in the vicinity of R = 1 the strength is clearly affected by imperfections. The strength is less than K_ℓ even when $K_E > K_\ell$. Since the strength depends on the amount of imperfection and even very small imperfections reduce the strength quite drastically, whereas the amount of imperfection of actual structures is unknown, the

strength of struts with R close to 1 cannot be established theoretically. One has to resort to compression tests and in order to account for scatter of the imperfections to do a series of tests on identical specimen.

4.2. The effect of "crushing"[8]

An in unloaded condition mathmatically straight strut can nevertheless be curved in the loaded condition. This phenomen is present when the strut or panel forms the compression side of a box beam. The box beam is curved when loaded in bending, more in particular with beams of small depth. Then the strut or panel supported on regularly spaced frames has to follow this curvature and is consequently loaded in bending. The end sections of one bay are rotated relative to each other. Consequently before buckling the strut is in a non-uniform state of strain, which means that its flexural rigidity varies along its length. This prebuckling state has the effect of reducing the strength.

The obvious parameter governing this reduction is the ratio of the radius of gyration (c in the present model) and the distance H of the member to the neutral plane of the box beam. In actual wing structure the practical limit ot j/H is about 0,1.

The investigation learned that with small j/H the reduction is proportional to $(j/H)^2$ therefore of little significance with $j/H < 0,05$. Also at $j/H = 0,1$ the additional reduction by j/H is inferior to the one by α, except when α is very small. E.g. with $\alpha = 1,25\%$ the the two reductions are about equal around $R = 1,2$.

These results, thereby recalling Gilbert and Calladine's conclusion on the more or less similar effect of excentricity, indicate that "crushing" needs not to be taken into account, nor any initial bending from other sources like surface loads of wing panels.

5. Local buckling confined to one side of the structure

The model considered in the preceding sections is very sensitive to mode interaction, and consequently to imperfections, due to the fact that upper and lower flange are both and equally subject to local buckling. When buckling occurs of a strut, comprising a number of bays separated by regularly spaced supports, the state of strain in the upper flange of one bay is equal to the state of strain in the lower flange of the next bay. Therefore the elastic line has its points of inflection precisely at the supports.

The situation is different when the crosssection is not symmetric. Asymmetry may be due to unequal flange imperfection with the previous model[2] or due to geometrical asymmetry of the crosssection. The latter condition is present in stringer reinforced skinpanels. This asymmetry causes different flexural rigidity for equal positive and negative curvature. Consecutive bays differ in flexural rigidity. Consequently the stiffer bays support the adjacent weaker ones.

A pronounced case of this type is the thin plate reinforced by stiffeners which do not participate in local buckling of the plate. It represents the lower extreme of the phenomen of mode interaction, in contrast to the previous model which is representative for the upper extreme.

Panels with large stiffener spacing have low local buckling stress of the plate. Their overall buckling stress is much greater. Therefore their buckling stress ratio R is far above unity. Then, as apparent from the previous model, K_b is far above K_ℓ. K_b is not affected by imperfections and can be established with the Euler formula thereby taking into account that the effective modulus of the plate is ηE.

When studying the possibility of unfavourable mode interaction attention can be restricted to panels with R close to unity. This inevitably means heavily reinforced panels, where stringer and plate sections are about equal. As a representative structure has been taken the case where the sections are equal. The results obtained with ratios between 1/3 and 3 are only slightly different.

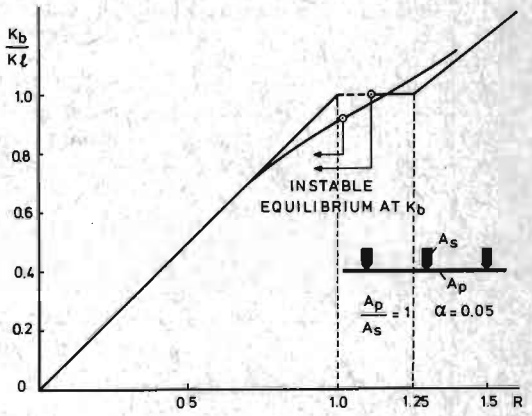

Figure 8. Panel buckling load K_b against K_E.

Fig. 8 shows the K_b/K_ℓ-R-curve for the perfect plate and for a plate with $\alpha = 0,05$.

With the perfect structure the reduction factor of the bending stiffness for $K_b > K_\ell$ is 0,8. This reduces the transition zone at $K_b = K_\ell$ to the range $1,0 < R < 1,25$. The equilibrium at $K_b = K_\ell$ is instable over the narrow range $1,0 < R < 1,11$. These upper limits are very low in comparison to those of the two-flange model where they are 2,45 and 1,725 respectively.

With the imperfection $\alpha = 0,05$ K_b is smaller than K_ℓ up to $R = 1,15$. The maximal reduction at $R = 1$ is 9%, whereas the two-flange model with $\alpha = 0,05$ has 17%.

Fig. 9 depicts the load-strain curve. Due to the large value of η_b (0,8) the kink in the curve for the perfect structure is only very weak: Consequently the curve for $\alpha = 0,05$ lacks a distinct rounded-off part. Again the slopes of the load-shortening curves at the bifurcation for $K = K_b$ are shown. The equilibrium at K_b is unstable, but the instability range of R has its upper limit at $R = 1,01$. The steepest tangent, which means the severest instability, occurs at $R = 0,85$ where $K_b/K_\ell = 0,814$. The maximal slope is however much milder than with the two-flange model. Consequently the sensitivity to column axis imperfection will be slight.

The conclusion can be that mode interaction and instability at the buckling load is confined to a very narrow region in the immediate vicinity of R = 1, where the buckling load is slightly below K_ℓ . The reason for this mild behaviour is that of two consecutive bays the buckling mode yields increased compressive strain in the skin of one bay and decreased strain in the adjacent one. So the bending stiffness of the first one decreases but it increases in the other one tempering the destabilization of the first one.

This concept leads to an important conclusion on the manner in which compression tests should be carried out when non-lineair behaviour of the structure occurs. Pin-ended columns or panels, though loaded in the centroid of the crosssection, will nevertheless be loaded in bending due to the gradual shift of the neutral axis whith increasing compressive strain. Test specimen of this kind will inevitably buckle with the concave side at the side most affected by non-linearity. Their failure load will be inferior to the buckling load. Compression tests should be carried out on specimen with rigidly clamped ends, taking their length twice the frame spacing. Then the point of application of the load before buckling moves with the neutral plane. For this reason the boundary conditions, assumed in the analysis, refer to clamped ends.

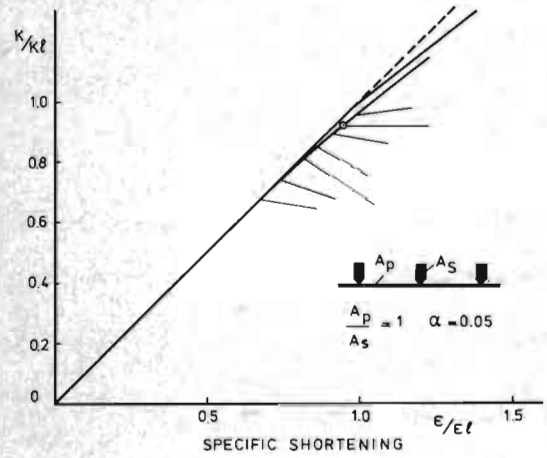

Figure 9. Load-strain curve of imperfect panel and tangents to the load shortening curve at the bifurcation load K_b.

6. Stiffened panels

6.1. Definition of the problem

The "extreme" cases discussed in sections 3, 4 and 5 were contrasting because the two-flange-model is equally affected by local buckling at both sides, whereas the other model was subject to local buckling only at one side. Real panels are situated somewhere between these two extremes. Their difference with the model of section 5 is that the top side of the stringer is subject to local buckling. Their difference with the two-flange model is that the topside of the stringer has much smaller crosssection than the opposite side of the panel structure and consequently affects the behaviour of the structure to a lesser degree. The problem is to locate their position between the "extreme" cases. Some research of this kind has been performed during recent years.

Tvergaard[9,10] investigated the integrally stiffened panel. The stiffeners have rectangular cross-section and their width is much larger than the plate thickness. The way is which the stiffeners distort due to local buckling of the plate is just torsion. The torional stiffness gives a fair amount of restraint at the edges of the plate strips and consequently the stiffener torsion is small. In so far the behaviour of this structure cannot differ much from that of the model of section 5. An important cause of difference is the fact that Tvergaard considers one single panel loaded in the centroid of its crosssection. Then the reduction of the strength is more severe than with clamped ends or with the multi-bay panel, as discussed in section 5. With clamped ends the incorporation of stiffener torsion will presumably yield results not much different from those obtained in section 5.

Still open is the question of the behaviour of panels with thinwalled stiffeners, such as have Z- or tophat section. Then local buckling distorts the cross section as well of the stringer as of the plate. The local buckling mode depends on quite a number of geometrical parameters. The crosssection consists of several plate strips of different width and thickness. The ratios of the widths and of the thicknesses are the determining parameters. The coherence of the strips requires equal longitudinal wave length of all strips, therefore different ratios of wave length and strip width. The fact that the strips buckle together means that their buckling stresses are equal. Consequently their buckling coefficients will be very different. Equality of wave length and buckling stress is being achieved by bending moments occuring between the strips at their junction. These moments can have a stabilizing effect (positive elastic restraint) or destabilizing effect (negative elastic restraint).

The investigation of mode interaction requires the determination of the local buckling mode and of K_ℓ. Methods are available.

Next comes the post-buckling behaviour of the perfect structure and the behaviour of imperfect structures. This is a very complex problem.

Let be assumed that the stiffness of edge restraints remains constant with increasing edge strain. Then the problem is to establish the stiffness of a strip in compression as function of the edge strain for arbitrary wave length and arbitrary edge restraint whereas these restraints at the two edges can have any ratio positive or negative. This is a cumbersome problem though its solution does not even solve the problem of panel behaviour under compression without bending, where all the edges have the same strain. The cause of this unsuffiency is that under the assumption of constant edge restraint the increase of the edge rotations with increased compression will be different for adjoining strips. So in fact the stiffness of edge restraint must vary with the edge strain so as to yield compatible edge rotations.

The need to establish the bending stiffness of the panel introduces an additional problem. Plate

strips not parallel to the panel plane have different edge strains due to panel bending. The location of the neutral plane is unknown and therefore the ratio of the edge strains. So the behaviour of plates with arbitrary ratio of edge strains, arbitrary wave length, ratio of edge restraints and amount of edge restraint would have to be investigated. These data are needed for solving the mode interaction problem of the stiffened panel. If they were available the remaining interaction problem would not be too cumbersome. The main problem is the one on strip behaviour just defined.

Recalling that ignorance of the amount of imperfections excludes the possibility to predict the strength of these structures exact solution of the problem seems to have little practical value and would be tooambitious. On the other hand it serves a real need to explore the extent of the range of R in which interaction presents reduced strength and the degree of importance of this reduction.

Therefore the logical step after having considered the two "extreme" models is to consider a model which is not identical to but representative of real panel structures, choosing the model such that the problem of the behaviour of its composing strips is not too complex.

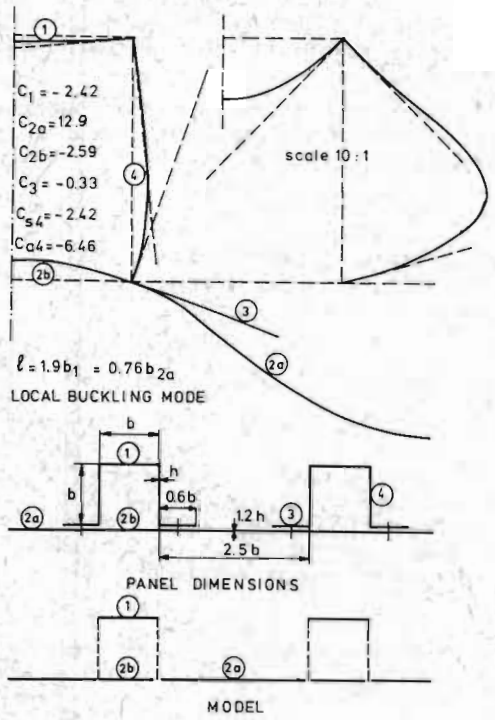

Figure 10. Local buckling mode of panel and simplified model of the panel.

6.2. The model of the panel

The selected structure is a panel stiffened by top-hat stringers (fig. 10). The ratio of strip width and thickness is arbitrary. The cross sections of plate and stringers are equal.

The local buckling strain has been established by means of a straightforward method[11] as

$$\varepsilon_\ell = 1{,}340 \frac{\pi^2}{12(1-\nu^2)} \frac{h^2}{b^2} .$$

The half wave length of the mode is 1,90 b. The mode shape and edge rotations are shown in fig. 10.

The joints of plate and stringer have been assumed in the intersection of the plate and the side strips of the stringer, whereas in the real structure the rivet joint will be somewhere near the centre of the flanges. With the joint along the rivet row the edge deflection of the plate strips would be non-zero, which would complicate the problem quite seriously. Another difficulty would be to deal with the flange loaded in the rivetline. However under these realistic conditions the deflections at the intersection of plate and side strips would be close to zero, as can be conjectured by inspection of fig. 10. Further considering that the flanges contribute only 14% to the total crosssection a rude approximation of their condition seems acceptable.

The kind of restraint offered to the edges of the strips appears from the curvature of the mode. Strip 2a clearly obtains support from plate strip 2b and stringer strip 4, these latter then having negative restraint. The upper edge of strip 4 is being restrained by strip 1. The figure also mentions the coefficients of restraint C defined by

$$\frac{\text{edge moment}}{\text{edge rotation}} = - C \frac{\text{bending stiffness of plate}}{\text{plate width}}$$

With strip 4 C_s and C_a refer to the symmetric and anti-symmetric part of the mode. The figures indicate that the wide plate strip 2a, being the weakest part of the structure, gets very stiff edge restraint from the adjoining strips.

The model selected for the analysis of mode interaction is for various reasons a simplified representation of the basic structure. Only those strips are represented which have symmetrical buckling mode: strips nr. 1, 2a and 2b. The flanges nr. 3 can be omitted since they contribute very little to the bending stiffness of the panel in comparison to the plate nr. 2. Also the axial load carried by the stringer sides nr. 4 is being neglected so as to avoid serious complications arising from unequal restraint stiffnesses at upper and lower edge and unequal edge strains with panel bending.
The function of the stringer sides to maintain the integrity of the assembly is being preserved. These omissions have only slight influence on the radius of gyration j; it increases from 0,377 b to 0,394 b.

The emphasis in this investigation falls on the effect of stiffness reduction of the stringertop nr. 1 as a rather small flange affected by local buckling.

A further simplification is that the coefficients of edge restraint C are assumed not to vary with the edge strains and remain equal to their value at local buckling, given in fig. 10. As demonstrated in section 6.1 the stiffness of edge restrains varies with the applied strain as well in compression as in bending of the panel. Moreover it depends on the imperfections assumed for the various strips. The aim of this investigation is to get some idea of the significance of mode interaction with stiffened panels and to answer the questions: what

is the range of the structural parameter R over which mode interaction reduces the strength; what is the order of magnitude of this strength reduction due to imperfections of the strips; what about the stability at the bifurcation and the effect of additional imperfection of the panel axis. For this kind of orientation in the problem a qualitatively correct representation of the behaviour of the structural elements seems acceptable. Then the assumption of edge restraint coefficients of the correct order of magnitude satisfies the purpose.

The wave length of the strip deformations is as established for local buckling.

Assumptions have to be made on the imperfections of the several strips. For obvious reasons they have been taken similar to their local buckling mode shown in fig. 10. The size of the imperfections however has no relation to the wave amplitude in local buckling. It has been assumed that the ratios of the initial deflections in the centre of the strips to the strip widths are equal for all three strips. Three degrees of imperfection have been chosen (Tabel I).

Table 1. Imperfections α = amplitude: strip thickness.

strip	I	II	III
1	0,012	0,024	0,036
2a	0,025	0,050	0,075
2b	0,010	0,020	0,030

6.3. The behaviour of elastically restrained strips

The tool required for establishing the bending stiffness of the model as defined in section 6.2 is the knowledge of the load-shortening relation of plate strips, supported along their edges and having symmetrical elastic restraint at those edges, and at prescribed wave length. This as well for the perfect as for the imperfect strips.

The governing parameters are the wave length parameter $\lambda = \ell/b$, the coefficient of restraint C, the imperfectionparameter α and the compressive strain parameter $\varepsilon/\varepsilon_\ell$. Instead of C will be taken the local buckling coefficient k defined by

$$\sigma_\ell = k^2 \frac{\pi^2 E}{12(1-\nu^2)} \left(\frac{h}{b}\right)^2.$$

The relation between C and k is

$$C = -2\pi \frac{k}{\lambda} \left(\beta \operatorname{Tgh} \frac{\pi}{2}\beta + \gamma \operatorname{tg} \frac{\pi}{2}\gamma\right)^{-1},$$

where $\beta = \frac{1}{\lambda}(k\lambda+1)^{\frac{1}{2}}$, $\gamma = \frac{1}{\lambda}(k\lambda-1)^{\frac{1}{2}}$.

The local buckling mode is

$$w = \omega h \frac{\operatorname{Cosh}\frac{\pi}{2}\beta \cos\gamma\eta - \cos\frac{\pi}{2}\gamma \operatorname{Cosh}\beta\eta}{\operatorname{Cosh}\frac{\pi}{2}\beta - \cos\frac{\pi}{2}\gamma} \sin\xi, \tag{6.1}$$

where $\xi = \pi x/\ell$, $\eta = \pi y/b$ and ωh is the amplitude of the deflection. The imperfection is given by

$$w_o = \alpha \frac{w}{\omega}, \tag{6.2}$$

its amplitude being αh.

The method by which the P/P_ℓ-$\varepsilon/\varepsilon_\ell$ relation has been obtained is in principle identical to the method used for establishing the behaviour of the simply supported plate strip with $\lambda = 1$[3]. It consists of assuming a deformation mode corresponding to the local buckling mode (6.1). This assumption approximates the behaviour of the strip very well in the small range of $\varepsilon/\varepsilon_\ell$ close to unity which occurs in this problem. Then the linear differential equation for the Airy stress function F can be solved exactly. Thereupon F en w are substituted into the differential equation stemming from the condition of equilibrium in the direction normal to the plate. Since w is an approximate solution, F and w do not satisfy this condition. The Ritz-Galerkin condition requiring minimal potential energy, yields for given α and $\varepsilon/\varepsilon_\ell$ the approximation of the deflection amplitude ωh.

The P-ε-relation so established is in parametric form, for Poisson's ratio $\nu = 0{,}3$,

$$\varepsilon/\varepsilon_\ell = \frac{\omega}{\omega+\alpha} + \tfrac{1}{2} A\omega(\omega+2\alpha), \tag{6.3}$$

$$P/P_\ell = \frac{\omega}{\omega+\alpha} + \tfrac{1}{2} B\omega(\omega+2\alpha), \tag{6.4}$$

where A and B are functions of λ and k.
The formulae (6.3,4) correspond to those for the simply supported strips. Contrary to the simply supported strip, where λ and k are single valued ($\lambda = 1$, $k = 2$), in this case λ and k can have any value. The derivation of A and B appears to be a very laborious operation. Also the formulae of A and B are so lengthy that their reproduction in this context is prohibitive. They will published separately[12].

From the formulae (6.3,4) follow the quantities η, η' and μ needed for establishing the behaviour of the model.

$$\eta = d(P/P_\ell)/d(\varepsilon/\varepsilon_\ell) = \frac{1+BX}{1+AX}, \tag{6.5}$$

$$\eta' = d\eta/d(P/P_\ell) = -\frac{3(A-B)XY}{\alpha(1+AX)^2(1+BX)},$$

$$\mu = \frac{1}{6}(2\eta'^2 - \eta\eta'') = -\frac{Y(4-5BX)\eta'}{6\alpha(1+AX)(1+BX)},$$

where $X = Y^3/\alpha$ and $Y = \omega+\alpha$.

The known values of λ and k of the strips yield the values of A and B, given in tabel II, together with B/A. The post-buckling stiffness of the perfect plate strips is $\eta = B/A$, because $X = \infty$. For comparison table II mentions these quantities also for simply supported strips at the given wave length parameter λ and at $\lambda = 1$.

Tabel II. Stiffness parameters A and B.

stripnr.	λ	C	k^2	A	B	η=B/A
1	1,90	-2,42	1,340	2,1183	1,5067	0,7113
2a	0,76	12,9	5,82	1,1722	0,4463	0,3807
2b	1,90	-2,59	0,931	4,370	3,476	0,7954
-	0,76	0	4,31	1,7402	0,6432	0,3696
-	1,00	0	4	1,1536	0,4710	0,4083
-	1,90	0	5,89	0,2726	0,1441	0,5288

It appears from the data for C = 0 that the post-buckling stiffness increases with λ. This is plausible because increased longitudinal waviness

(smaller λ) makes the strip more flexible, thus reducing its stiffness. Comparing the figures for $C = 0$ and $C \neq 0$ it appears that for $\lambda < 1$ $C > 0$ yields a slight increase of η, whereas for $\lambda > 1$ $C < 0$ yields considerable increase of η.

The load-strain curves of the strips for $C \neq 0$, $\alpha = 0$ are shown in fig. 11.

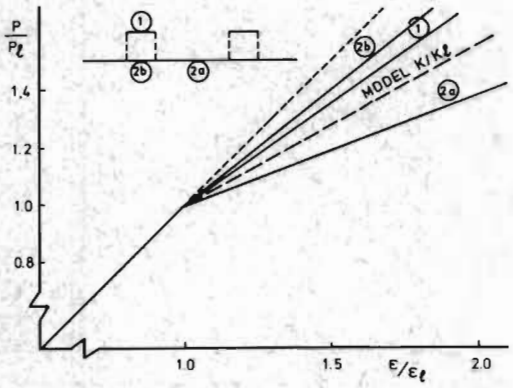

Figure 11. Load-strain curves of composing plate strips and model.

6.4. The buckling load of the perfect model

The crosssection of a strip i is $A_i = F_i A$, where A is the total cross section of the model. The stiffnesses of strips 2a and 2b can be combined to a single stiffness of a flange 2 with the cross-section $A_2 = A_{2a} + A_{2b}$:

$$(\eta F)_2 = (\eta F)_{2a} + (\eta F)_{2b}. \qquad (6.6)$$

Then the bending stiffness of the model is

$$\eta_b EI = \frac{(\eta F)_1 . (\eta F)_2}{(\eta F)_1 + (\eta F)_2} EAc^2.$$

Since

$$EI = \frac{F_1 F_2}{F_1 + F_2} EAc^2$$

and by definition $F_1 + F_2 = 1$

$$\eta_b = \frac{\eta_1 \eta_2}{(\eta F)_1 + (\eta F)_2} \qquad (6.7)$$

From fig. 10 follows $F_1 = 1/5{,}2$, $F_{2a} = 3/5{,}2$, $F_{2b} = 1{,}2/5{,}2$. Then the η's given in tabel II yield $\eta_2 = 0{,}4992$ and $\eta_b = 0{,}6576$. (fig. 11)
Fig. 12 gives $K_b/K_\ell = \eta_b R$. (6.8)

The panel length $2L_o$ (the parameter R_o), at which the model is in neutral equilibrium at the load K_ℓ, can be established as follows (fig. 13).

The buckling mode consists of a part of length L_I, where flange 1 is at the concave side of the mode, and of the two parts of length $\frac{1}{2} L_{II}$, where flange 2 is at the concave side. Since before buckling the strain is just ε_ℓ, the part L_I has $\eta_1 = 0{,}7113$, $\eta_2 = 1$, and the part L_{II} has $\eta_1 = 1$, $\eta_2 = 0{,}4992$. At the transition of parts L_I and L_{II} the bending moment vanishes. The parts L_I and L_{II} can be considered to be pin-ended columns and their buckling

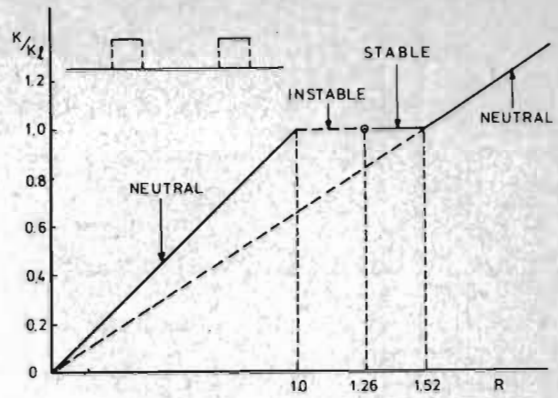

Figure 12. Buckling load K_b of perfect model.

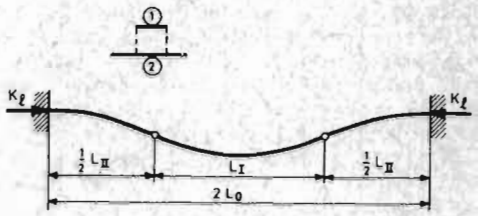

Figure 13. Overall buckling mode of panel at R_o.

loads are equal. Then L_I^2 and L_{II}^2 are proportional to the bending stiffnesses of the two parts.

The bending stiffness reduction factors of the two parts following from (6.7) are $\eta_I = 0{,}7531$, $\eta_{II} = 0{,}8383$.

$$2L_o = L_I + L_{II} = L_I\left[1+\left(\frac{\eta_{II}}{\eta_I}\right)^{\frac{1}{2}}\right],$$

$$K_b = K_{b_I} = \eta_I \frac{\pi^2 EI}{L_I^2} = \tfrac{1}{4}(\eta_I^{\frac{1}{2}} + \eta_{II}^{\frac{1}{2}})^2 \frac{\pi^2 EI}{L_o^2} =$$

$$= \tfrac{1}{4}(\eta_I^{\frac{1}{2}} + \eta_{II}^{\frac{1}{2}})^2 (K_E)_o.$$

Since $K_b = K_\ell$

$$R_o = 4(\eta_I^{\frac{1}{2}} + \eta_{II}^{\frac{1}{2}})^{-2} = 1{,}258.$$

The instable range of R ($1 < R < 1{,}258$) appears to be much smaller than with the two-flange model ($1 < R < 1{,}725$) but greater than with the panel where only the plate is subject to local buckling ($1 < R < 1{,}11$).

6.5. The buckling load of the imperfect model

At a given $\varepsilon/\varepsilon_\ell$, equal for the 3 strips, follows from (6.3) their ω, or better Y by rewriting (6.3) as $Y^3 + \left[(1-\varepsilon/\varepsilon_\ell)\, 2/A - \alpha^2\right]Y - 2\alpha/A = 0$. (6.9)
Thereupon (6.5) yields their η and next (6.6,7) yield the reduction factor of the bending stiffness η_b.

$$P_{\ell i} = F_i K_\ell,$$

$$K_b = \Sigma P_i = \Sigma (P/P_\ell)_i F_i K_\ell. \qquad (6.10)$$

$(P/P_\ell)_i$ follows from (6.4), then K_b/K_ℓ is known for the chosen value of $\varepsilon/\varepsilon_\ell$. Thereafter R pertaining to K_b/K_ℓ follows from (6.8). The K_b/K_ℓ - R curves for the three cases of imperfection, defined in tabel I, are shown in fig. 14.

The maximal reductions of the buckling load, occurring at $R = 1$ are resp. 9, 12,5 and 14%. For $R > 1{,}35$ K_b exceeds K_ℓ. With R close to unity the strength reduction by strip imperfection appears to be not negligible.

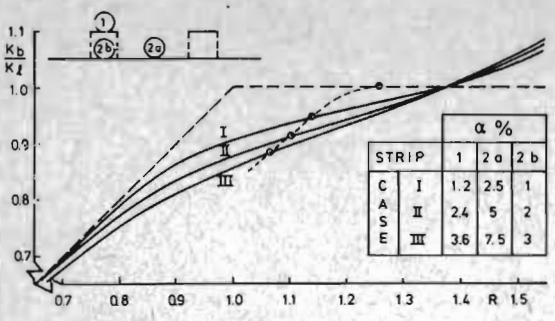

Figure 14. Buckling load K_b of imperfect models.

6.6 The character of the equilibrium at K_b

The derivation of the differential equation representing the condition of equilibrium at small finite deflections is similar to the one given in section (3.2) for the two-flange model. Due to the lack of symmetry of the model the expression for the bending moment contains also a term of the second degree in V''. The coefficients appearing in M have of course a greater complexity, being functions of $R, \eta_i, \eta_i', \mu_i, F_i$ $(i = 1, 2a, 2b)$.
The differential equation corresponding to eq. (3.12) reads

$$\left\{V''\left[1+A_1\frac{R}{\rho}V''-(A_2-2A_1^2)\frac{R^2}{\rho^2}V''^2-A_3\frac{1}{4\rho}tV_o^2\right]+\right.$$
$$\left.+\left(1+\frac{1}{4\eta_b R\rho}tV_o^2\right)\right\}'' = 0, \quad (6.11)$$

where $\rho = j^2/c^2 = F_1F_2$, $V = W/c$.

Hence $(W_o/2j)^2 = V_o^2/4\rho$, and A_1, A_2, A_3 are rather complicated functions of the stiffness characteristics of the strips, η, η' and μ, pertaining to ε_b.

$$A_1 = (-\gamma_2^2\phi_1 + \gamma_1^2\phi_2)/(\gamma_1+\gamma_2)^2,$$

$$A_2 = (\gamma_2^3\mu_1 + \gamma_1^3\mu_2)/(\gamma_1+\gamma_2)^3,$$

$$A_3 = 2(\gamma_2\phi_1 + \gamma_1\phi_2)/(\gamma_1+\gamma_2)^2,$$

where

$$\gamma_1 = \eta_1F_1,\ \gamma_2 = \gamma_{2a}+\gamma_{2b} = (\eta F)_{2a} + (\eta F)_{2b},$$

$$\phi_1 = -\tfrac{1}{2}\eta_1',\ \phi_2 = -\tfrac{1}{2}\left[(\eta'\gamma)_{2a} + (\eta'\gamma)_{2b}\right]/\gamma_2,$$

$$\mu_2 = \left[(\mu\gamma)_{2a} + (\mu\gamma)_{2b}\right]/\gamma_2 - \tfrac{1}{2}(\eta'_{2a} - \eta'_{2b})^2/\gamma_2^2.$$

The solution of (6.11) for the clamped panel of length 2 L is

$$V = V_{10}(\cos\pi\frac{x}{L}+1) + \frac{1}{6}A_1\frac{R}{\rho}V_{10}^2(\cos 2\pi\frac{x}{L} - 1) +$$
$$+\frac{1}{32}(A_2+\frac{2}{3}A_1^2)\frac{R^2}{\rho^2}V_{10}^3(\cos 3\pi\frac{x}{L}+1) \quad (6.12)$$

and

$$t = \left[\frac{d\,K/K_\ell}{d(W_o/2j)^2}\right]_b = -\tfrac{3}{4}\,\frac{A_2 - \frac{10}{9}A_1^2}{\frac{1}{\eta_b R}+A_3}\cdot\frac{R^2}{\rho}. \quad (6.13)$$

The slope of the load-shortening curve at the bifurcation is

$$\left[\frac{d\,K/K_\ell}{d(-\Delta L/L\varepsilon_\ell)}\right]_b = \left\{(\gamma_1+\gamma_2)\left[1-\frac{1}{3}\gamma_1\gamma_2\frac{(\frac{1}{\eta_b R}+A_3)^2}{A_2-\frac{10}{9}A_1^2}\right]^{-1}\right\}_b \quad (6.14)$$

The load-shortening curves for the three cases of imperfection, defined in table I, together with the tangents at the bifurcation are given in fig. 15.

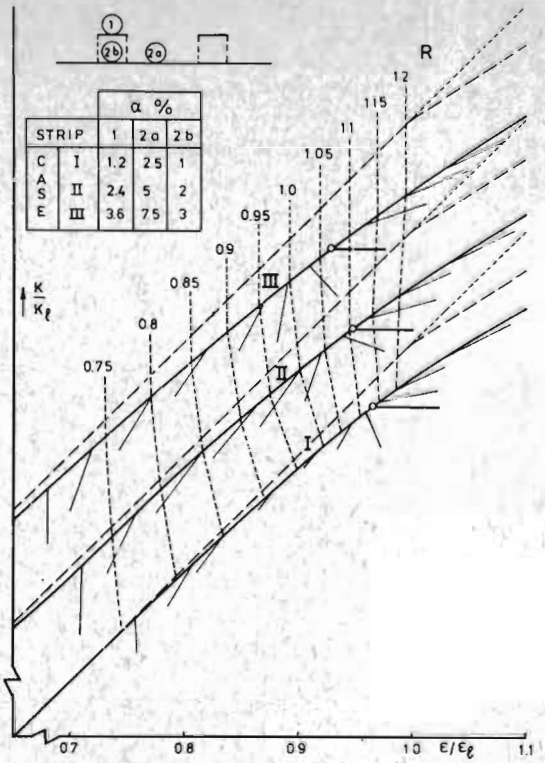

Figure 15. Load-strain curves of imperfect models and tangents to the load-shortening curves at the bifurcation load K_b.

The equilibrium at K_b appears to be unstable for $R<1,1$. In comparison to the "extreme" cases (figs. 6 and 9) the peaks of the load shortening curves are much sharper for this panel model. It implies that a panel without imperfection of the panel axis would fail explosively at K_b when the geometrical parameter $R<1,1$. Presumably it does not imply that the panel is more sensitive to axis imperfection than the two-flange model (section 4.1) More significant for this effect is the negative slope t given by (6.13).

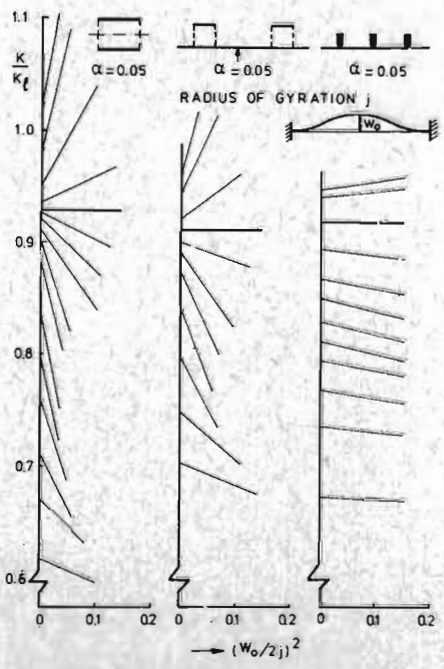

Figure 16. $d(\frac{K}{K_\ell})/d(\frac{W_o}{2j})^2$ at the bifurcation load K_b of three models

Fig. 16 compares these slopes of case II (α_{2a}=0,05) with the slopes of the extreme cases, both at α = 0,05. It appears that the lower extreme case (section 5) is almost insensitive to axis imperfection. The maximal slope with the panel model is half of the maximal slope with the two-flange model, not only in case II but as well for the cases I and III when compared with the two-flange model for $\alpha=\alpha_{2a}$ (Table III). The maximal

Table III. Comparison of maximal post-buckling slopes t.

case	$\alpha=\alpha_{2a}$	panel model	two-flange model
I	0,025	- 3,0	- 5,6
II	0,05	- 1,31	- 2,65
III	0,075	- 0,74	- 1,6
-	0,10	-	- 1,1

slope in case II is about equal to that of the two-flange model at α = 0,10, where axis imperfection adds little to the strength reduction.

As appears from fig. 7 the effect of axis imperfection extends into the range of R where the equilibrium at K_b is stable. Before reaching the stable load level K passes through the region where the stiffness characteristics - in particular the positive μ - are such that the structure responds with large deflections to the initial curvature. Deflection reduces the bending stiffness. It exhausts the load carrying capacity at $K<K_b$. So as yet the question is unanswered up to which value of R axis imperfection affects the strength unfavourably. It is intended to analyse this effect. As a tentative conclusion it might be conjectured that for R >1,35, where K_b exceeds K_ℓ, the effect of small axis imperfections will be negligible.

7. Conclusions

The value of the geometric parameter R is decisive for the loss of compressive strength of reinforced panels due to interaction of the local and the overall buckling modes. The detrimental effect of mode interaction is maximal at R = 1, the structure commonly considered to be optimal. When R >> 1 the stiffeners are negligibly little affected by local buckling. Then the effective bending stiffness can be established taking into account the post-buckling stiffness of the plate at large $\varepsilon/\varepsilon_\ell$. This procedure based on the "effective width" -concept is established practice. The effect of imperfections is neglible.

When tophat stiffened panels have R > 1,35 the imperfections: initial waviness of the thin walls and initial curvature of the panel axis have negligible effect on the compressive strength. However the buckling load K_b depends on the post-buckling characteristics of the entire structure: plate and stiffeners. This means that the determination of K_b requires knowledge of the bending stiffness of the panel in the post-buckling state. This problem is as yet unsolved.

At R<1,35 K_b is smaller than both Euler and local buckling load; the reduction depends on the amount of initial waviness and to some, presumably less, extent on axis imperfection. The maximal reduction by initial waviness, occuring at R = 1, is in the order of 10%. The additional reduction by axis imperfection has not yet been established. There are reasons to suspect that this addition reduction is not significant.

Scatter of imperfections with tophat-stiffened panels where R is between, say, 0,7 and 1,35 yi scatter of compressive strength. The strength o these structures cannot be predicted with great precision. Tests on a number of identical speci have to be carried out.

The strength of pin-ended panels is not represe tative of the strength of multi-bay panels. The position of the neutral plane shifts with incre sing compressive strain away from the side of t plate, causing bending before buckling, thereby lowering the failure load. Tests should be carr on clamped specimen.

References

1. A. van der Neut: The interaction of local bu ling and column failure of thin-walled compr sion members. Delft Un. of Techn., Dept. of Aer. Eng., Rep. VTH-149 (1968). In: Proc. 12 Int. Congr. Appl. Mech., pp. 389 to 399, Springer 1969.
2. J.J. Meyer and A. van der Neut: The interact: of local buckling and column failure of impe: fect thin-walled compression members. Rep. VTH-160 (1970).
3. A. van der Neut: The longitudinal stiffness c simply supported imperfect plate strips. Rep. VTH-152 (1968).
4. W.T. Koiter and G.D.C. Kuiken: The interactic between local buckling and overall buckling o the behaviour of built up columns. Delft Un. of Techn., Dept. of Mech. Eng., Rep. WTHD-23 (1971).
5. J.M.T. Thompson and G.M. Lewis. On the optimu design of thin-walled compression members. J. Mech. Phys. Solids 1972, Vol. 20, pp. 101 to 109.
6. R.B. Gilbert and C.R. Calladine: Interaction between the effects of local and overall impe: fections on the buckling of elastic columns. Un. of Cambridge, Un. Eng. Dep. (1973) (Submitted. to J. Mech. Phys. Solids).
7. A. van der Neut: The sensitivity of thin-walled compression members to column axis imperfection. Rep. VTH-172 (1972), In: Int. J. Solids and Struct. 1973, Vol. 9 pp. 999-1011, Pergamon Press.
8. A. van der Neut: Column failure of thin-walled compression members in aircraft wings as affec ted by wall imperfection and crushing. Rep. VTH-175 (1973).
9. V. Tvergaard: Imperfection sensitivity of a wide integrally stiffened panel under compression. The Danish center for Appl. Math. and Mech., Techn. Un. of Denmark, Rep. 19 (1971).
10. V. Tvergaard: Influence of post-buckling on optimum design of stiffened panels. Rep. 35 (1972).
11. A. van der Neut: The local instability of compression members built up from flat plates. Rep. VTH-47 (1952). In: C.B. Biezeno Annivers: ry Volume on Appl. Mech. 1953,pp. 174 to 197 Techn. Uitgeverij H. Stam.
12. A. van der Neut: The longitudinal stiffness o imperfect plate strips at arbitrary wave leng and symmetric edge restraint (1974) (To be published).

(May 1974)